Chapter 3

Transoral Robotic Surgery Applied to the Skull Base

Dorian Chauvet and Stephane Hans

Additional information is available at the end of the chapter

http://dx.doi.org/10.5772/intechopen.81048

Abstract

Skull base surgery has been developed with transsphenoidal approaches to reach the sella and especially the pituitary tumors. Transnasal endoscopic technique has become the gold standard for many years. Indeed, the intraoperative view with specific endoscope is very good, and thus the gross total of pituitary adenomas removal rates have been increased. Nevertheless, why has not this technique been challenged, especially given the potential rhinologic side effects and 2D vision? Robotic surgery with the da Vinci system is now well known all over the world. Transoral robotic surgery (TORS) is also commonly used in head and neck cancer with satisfying results. In this ENT approach, the da Vinci videoendoscope looks downward; we had the idea to place it behind the hard palate in order to look upward. Therefore, from cadaveric studies to clinical "première mondiale," we developed an innovative TORS to reach the sella and to remove pituitary tumors.

Keywords: transoral robotic surgery, pituitary adenoma, da Vinci system, skull base surgery, robot-assisted surgery, transsphenoidal surgery

1. Introduction

Initial attempts at transsphenoidal surgery were first tested at the beginning of the twentieth century by early neurosurgeons [1]. Over the past 30 years, endoscopic transnasal techniques have become the gold standard, avoiding scares and allowing a better field of vision into the nasal narrow corridor. However, endoscopic approaches continue to present several inconveniences such as the narrowness of the operative corridor, the potential rhinologic side effects after removal of endonasal structures (such as turbinates or nasal septum), the two-dimensional vision, and a quite long learning curve. One could also mention the ergonomic

discomfort for the surgeon to perform fine dissection requiring two hands compared to microscopic classic dissection.

For many years, robotic surgery with the da Vinci system (Intuitive Surgical Inc., Sunnyvale, CA, USA) has been increasingly adopted, especially in urology [2] and gynecology [3]. This system offers increased freedom of movement within narrow corridors, three-dimensional visualization, motion scaling, and tremor filtration [4]. Moreover, the ergonomic comfort for the surgeon has improved. Recently, robot-assisted surgery has been performed for pharyngeal and laryngeal cancers in a minimally invasive perspective [5–7], leading to a new concept of *transoral robotic surgery* (TORS).

Concerning the neurosurgical field and especially the skull base field, literature with da Vinci surgery remains very poor, including a few cadaveric odontoidectomies [8–10] and one case report [11]. Moreover, it has to be mentioned that robotic supratentorial approaches by keyhole craniotomies have failed on cadavers [12].

In 1985, Crockard wrote that "the transoral surgical approach allows access to structures from the sphenoid sinus rostrally to the fourth cervical vertebral body caudally" [13]. Despite this pioneer reference and the new technical opportunities given by robot-assisted surgery, no TORS has been attempted to reach the sella turcica. Thus, we developed an innovative TORS for skull base in three steps: cadaveric study [14], anatomical general work [15], and clinical proof of concept [16].

2. Cadaveric study

2.1. Methods

Dissections were performed at the "Ecole Européenne de Chirurgie" with the da Vinci S HD 4 arms system. Regarding the anatomical consideration, only three arms were used (videoendoscope arm and two instrument arms). The system stood at the head of the cadaver, placed supine next to a C-arm fluoroscope (operative room plan in **Figure 1**).

A mouth retractor (type Doyen, Landanger®) was placed to get the usual transoral exposition. The soft palate was retracted using two rubber catheters introduced into the nose and pulled out by the mouth. Additionally, the tongue could be retracted with a stitch as well. An 8.5-mm 30° angled binocular endoscope, a 5-mm EndoWrist® Maryland dissector articulated, and a 5-mm EndoWrist® Monopolar cautery instrument were attached on the patient cart, respectively, on the middle, right, and left arms of the system. The three arms were brought into the oral cavity: the 30° videoendoscope arm facing upward on the midline and the two other robotic arms laterally, respecting teeth and labial commissures of the mouth (see **Figure 2**).

It is mandatory to mention that two surgeons were necessary to perform the dissection: one author, head and neck surgeon (SH), at the console and the other one, neurosurgeon (DC), at the bedside. The latter was necessary to perform suction and to prevent a robotic arm conflict with the oral cavity structures during the mucosal dissection. Afterward, the second surgeon performed the bone drilling and the sellar opening. Four phases can be defined:

http://dx.doi.org/10.5772/intechopen.81048

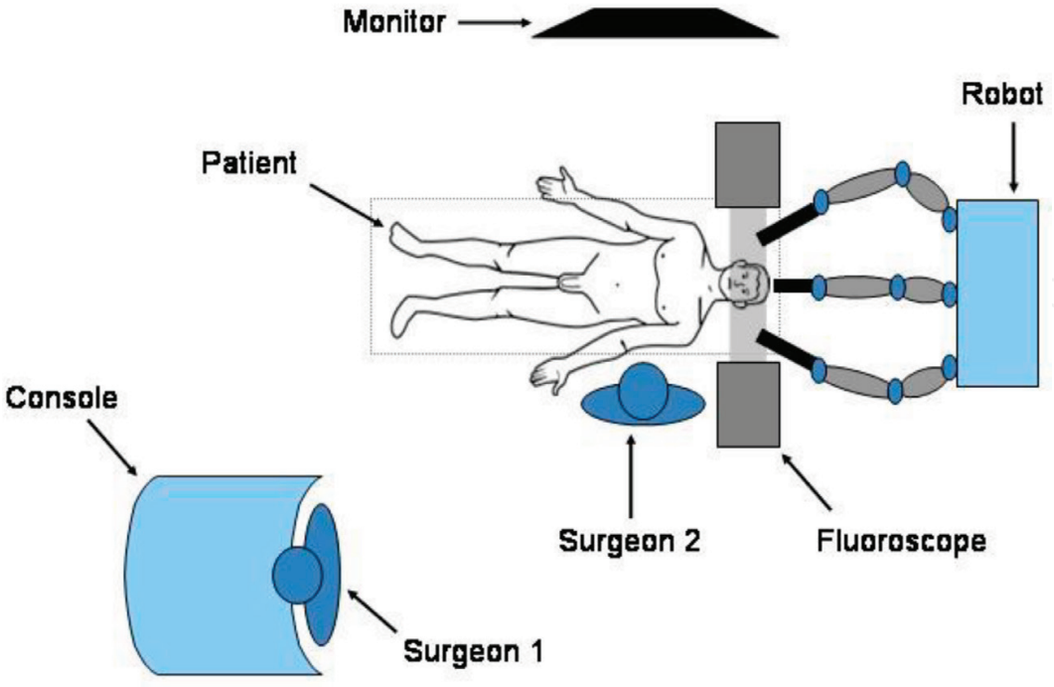

Figure 1. Schematic view of the operating room. Surgeon 1 is the head and neck surgeon working at the console (SH) and Surgeon 2 is the neurosurgeon working at the bedside (DC) [14].

Figure 2. Lateral intraoperative view. The three robotic arms stand in the oral cavity that is open with a mouth retractor. The retraction of the soft palate is performed using two rubber catheters introduced in the nose and pulled out by the mouth. In the background, the C-arm fluoroscope for intraoperative 2D lateral control [14].

2.1.1. Mucosal time

Once the endoscope was pushed beyond the hard palate, an upward view of the cavum and the choanae was obtained. The surgeon at the console performed the flap of the posterior cavum mucosa, which corresponded to the mucosa covering anteriorly and inferiorly the sphenoidal rostrum (see **Figure 3**).

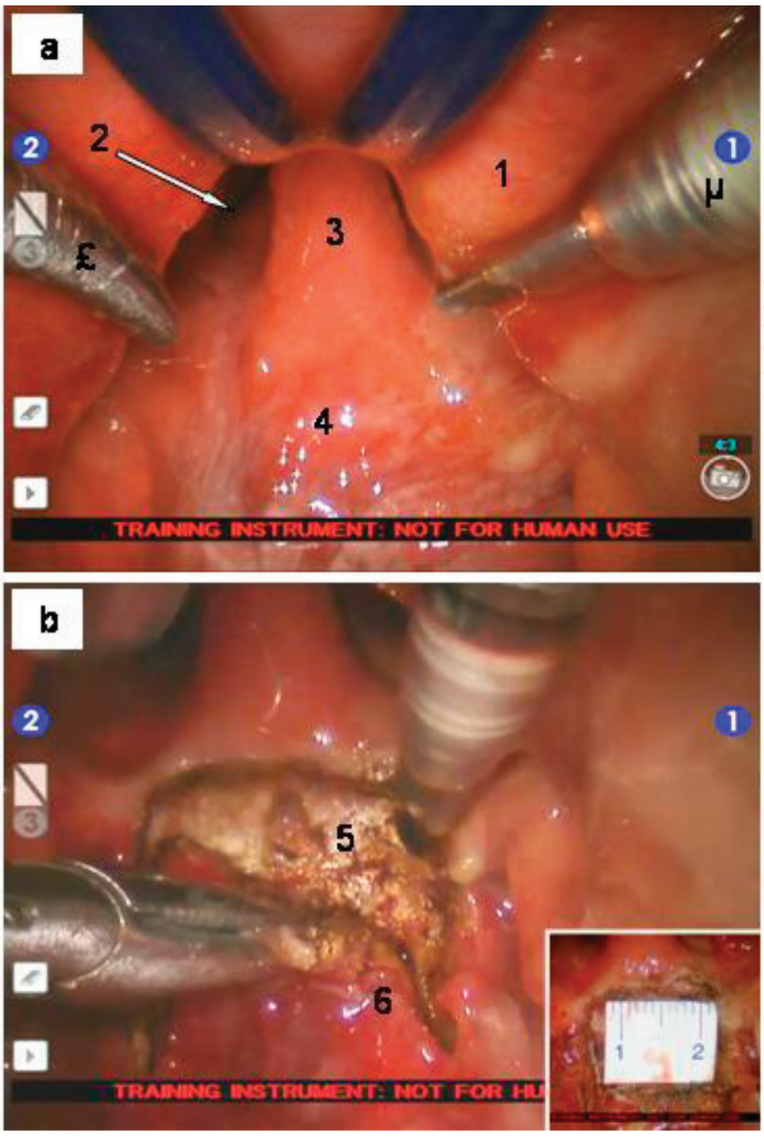

Figure 3. Intraoperative view with the 30° endoscope within the cavum. (a) The soft palate (1) is retracted using two rubber catheters at the top of the picture. The choanae are well visualized (right choana) (2). (3) indicates a decisive landmark that corresponds to the articulation between the vomer and the sphenoid. (4) is the mucosa of the cavum and (μ) and (£) are monopolar cautery and Maryland dissector, respectively. (b) The mucosal flap (6) is dissected with a caudal base in order to discover a key point that corresponds to the junction between the alea of the vomer (5) and the sphenoid itself; the picture on the right bottom corner indicates the size of the flap, approximately 15 mm width [14].

2.1.2. Sphenoid time

Afterward, the surgeons' roles changed, and the left robotic arm was removed to provide space to the neurosurgeon at the bedside. As the da Vinci system has no bony instruments, the opening of the sphenoid sinus was performed by the neurosurgeon, watching his progression on the 2D flat-panel screen. The first surgeon sitting at the console offered a supplementary intraoperative control with 3D view and could perform suction thanks to a dedicated robotic tool—8 mm EndoWrist® One™ suction irrigator. An electric motor (Bien-Air®) was employed with matchstick burs attached on a slightly angled handpiece. Another drilling system was employed in the clinical study (see below) [16]. Before drilling the sphenoid, the attack angle

of the drill was verified by a lateral fluoroscopy. The sphenoid sinus was opened and enlarged with kerrison punch to get a wide vision of the sella turcica (see **Figure 4**).

2.1.3. Sellar time

The sellar floor was opened with the drill and the kerrison punch. The robotic arms were inserted into the sphenoid sinus deeply to appreciate the maneuverability of the da Vinci EndoWrist® instruments in such a narrow space. The dura mater opened the robotic monopolar cautery. In clinical study [16], other instruments were used to open the dura (see below). The pituitary gland resection of the cadavers was attempted, and anatomical suprasellar structures were identified (see **Figure 5**).

2.1.4. Closure

Suture of the flap was attempted.

Times of each step were assessed and unexpected difficulties were reported.

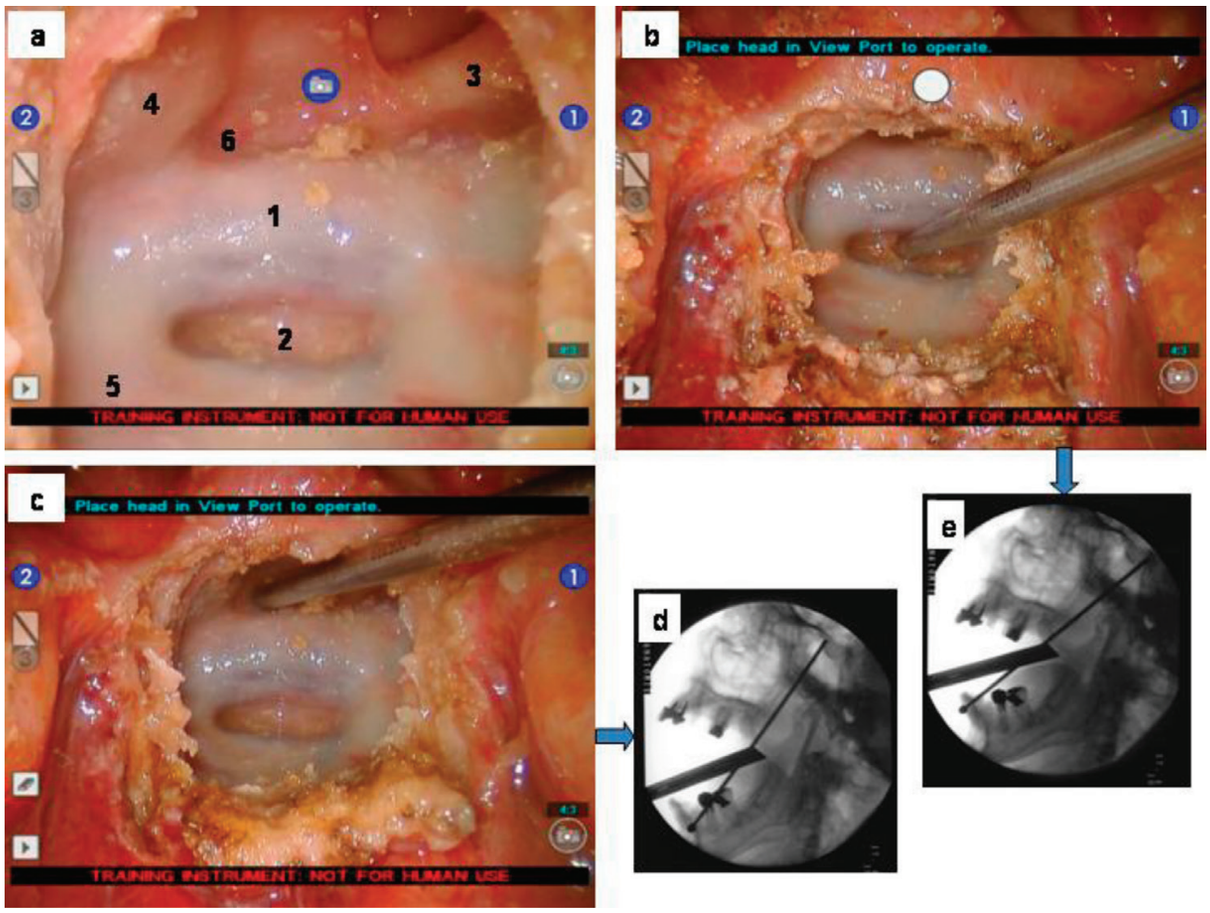

Figure 4. Intraoperative endoscopic view of the sella turcica. (a) Anatomical structures of the sphenoid sinus: (1) sellar floor, (2) dorsum sellae that is well pneumatized, (3) left optic nerve protuberance, (4) right carotid protuberance—sellar portion, (5) right carotid protuberance—clival portion, and (6) opto-carotid recess. (b) Dissector placed in the pneumatized dorsum sellae and the corresponding fluoroscopic lateral picture (e). (c) Dissector inserted in front of the anterior wall of the sella and the corresponding fluoroscopic view (d) [14].

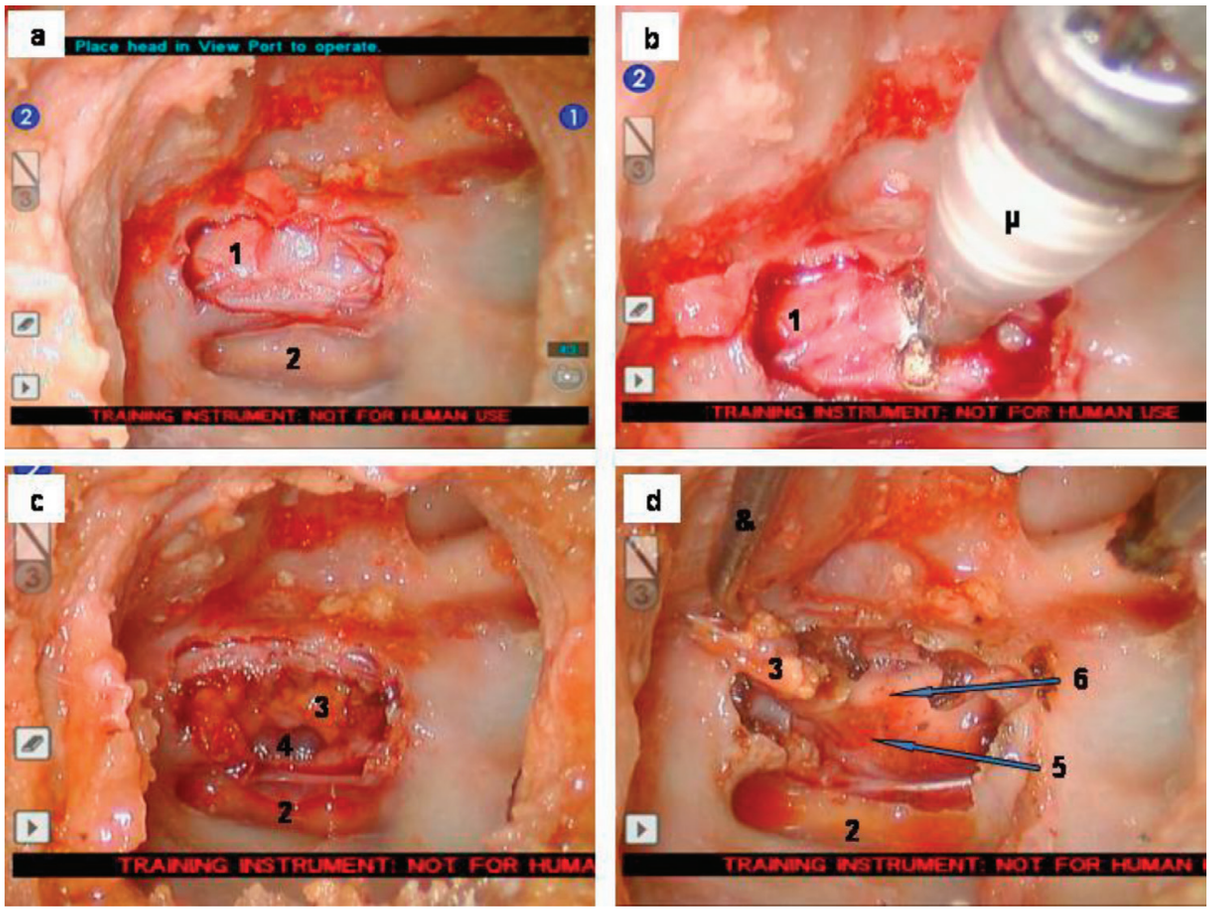

Figure 5. Intraoperative view of the pituitary fossa dissection. (a) View after sellar floor removal. (b) Cauterization of the sellar dura with the monopolar cautery (μ). (c) View during pituitary gland resection. (d) Final view after removal. Legends: (1) sellar dura, (2) pneumatized dorsum sellae, (3) pituitary gland, (4) sellar diaphragm, (5) pituitary stalk retracted by a hook (6), and (7) optic chiasm [14].

2.2. Results

A total of 11 cadavers were dissected. Despite the anatomical heterogeneities of the specimens, the setup was easy, and the visualization of the cavum was large with a perfect view. At that time, two structures were required as reference points: both sides of choana and the posterior border of the vomer that provided an accurate midline landmark. As in other transsphenoidal approaches, keeping the dissection on the midline was mandatory. We did not experience lateral deviation in our dissections. The cavum mucosa was not always dissected in a whole flap (n = 5) as tissues of cadavers were sometimes fragile. All of the soft tissue sequence was performed easily with enough space to use the robotic instruments and without any tension on the oral cavity structures, especially the soft palate. Once the mucosal flap was raised, we defined a key point to enter the sphenoid sinus, which corresponded to the junction between the vomer and the sphenoid itself (see **Figure 3**).

All sphenoidal sinuses were "sellar," which meant that the pneumatization was posterior to the anterior wall of the sella turcica. The bony sequence was achieved by placing the motor handpiece in the right labial commissure of the mouth. Indeed, the lateral movement of the handpiece, following naturally the lower teeth curve from the midline to the labial

commissure, allowed an opening of the angle of work to the skull base (see **Figure 6**). The latter was defined by the angle between the horizontal line passing through the hard palate and the projected line of the drill (as seen in **Figure 6** by dotted lines), which was placed at the midline and then in the labial commissure. From these comparative cadavers' measurements, we observed that the mean angles of work were 55° (min 48, max 62) and 71.5° (min 67, max 76) for the midline and the lateral positions, respectively. Thus, we hypothesized that the mean angle of work gain placing the drill in the labial commissure was +16.5°.

In all dissections, this procedure had succeeded in approaching the sella turcica, and we had encountered no difficulty in our approach. To prevent a lateral deviation of the drilling, the angled feature of the handpiece was decisive. Opening the sphenoid sinus was achieved quickly (approximately 10 min), depending on the thickness of the sphenoidal rostrum. The videoendoscope was successfully introduced in this sinus during all dissections and thus had provided a wide 3D view of the sella turcica and its surrounding structures (as shown in **Figure 5**). Then, the pituitary fossa was opened with a thinner diamond drill. The robotic arms reached the sella turcica in all procedures with a correct manageability. The normal pituitary gland was removed with robotic instruments (see **Figure 7**). The final view of the pituitary stalk and the optic chiasm was obtained. Closure attempts to suture the dura were impossible, and it was quite difficult to suture the flap due to the fragile mucosa. At the end of the dissection, inspection of the oral cavity revealed no injury. The mean robotic setup time was 20 minutes (range, 10–35 minutes); the mean mucosal time was 10 minutes (range, 5–15 minutes); and the combined sphenoid and sellar time was 30 minutes (range, 15–60 minutes).

In conclusion these cadaveric preliminary results were very promising and TORS skull base seemed reproducible, awaiting further clinical trial.

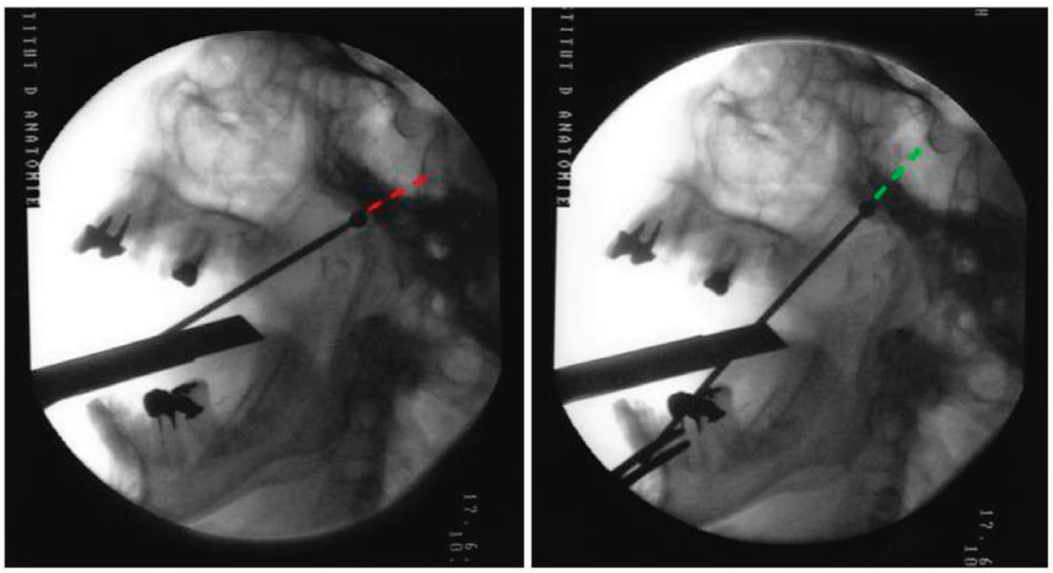

Figure 6. Fluoroscopic lateral views, the endoscope standing at the midline of the mouth. On the left, the matchstick drill is inserted at the midline, and its projection on the sphenoid bone virtually meets the clivus (red-dotted line). On the contrary on the right picture, the bur is placed in the labial commissure, and its projection clearly meets the sella turcica (green-dotted line). This shows how the angle of work to the skull base is increased when the instruments are placed laterally in the oral cavity [14].

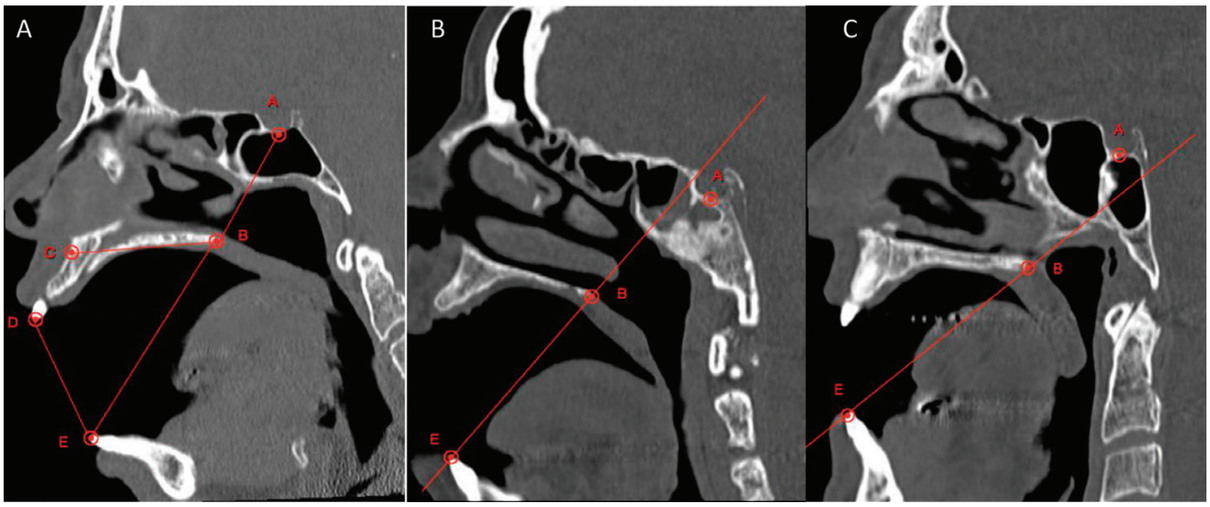

Figure 7. CT scan bony window sagittal midline views. (A) Description of the different points: A, sella turcica point; B, posterior palatine point; C, anterior palatine point; D, maxillary dental point; and E, mandibular point. Notice that the (BE) line is projected on point A on this picture. (B) Presellar projection of (BE) line. (C) Postsellar projection of (BE) line [15].

3. Anatomical study

3.1. Methods

This prospective single-center study hypothesized that TORS for skull base would be feasible in the majority of patients, regardless of their anatomical features [15]. Thus, we studied some anatomical criteria on radiological data from patients requiring a cerebral CT scan for neurological issues. Patients were asked to open their mouth as large as they could during the CT scan, without any retractor. Patients with a history of endonasal surgery, sinus disease, and/or skull base pathology were excluded. After imaging acquisition, we also excluded patients with mouth opening inferior to 30 mm, as this threshold distance was far from the value with the usual mouth retractor [14]. CT scans were performed on a Somatom 16, Siemens. A double lecture was performed by one neurosurgeon and one neuroradiologist, who both collected the following data.

Firstly, on a sagittal midline view, we defined five points for each patients corresponding with strategic landmarks (see **Figure 7**), such as:

- Point A: the lowest point of the sella turcica.
- Point B: the most posterior palatine bone point.
- Point C: the most anterior palatine bone point.
- Point D: the maxillary dental point, at the tip of superior incisor.
- Point E: the mandibular dental point, at the tip of inferior incisor.

CT measurements also included four distances between the previous points, such as:

- [DE] for mouth opening
- [BC] for the length of the palate
- [AB] for the distance between the posterior edge of the palate and the sella
- [BE] for the distance between inferior incisors and posterior edge of the palate

Then, we examined from these landmarks the projection of the dental palatine line (aka (BE) line) on the sella. Patients were classified in three categories: projection anterior to point A of the sella (aka presellar projection), on point A, and posterior to point A (aka postsellar projection) (see **Figure 7A–C**, respectively). Finally, the alpha angle, named α, was determined as the angle between the horizontal palatine (BC) line and the dental palatine (BE) line (see **Figure 8A** and **B**).

Secondly, a 25° rotation from point B was made on the axial view to obtain a parasagittal oblique view (see **Figure 8C** and **D**) that corresponded to a specific intraoperative plane (see **Figure 8E**). Indeed, this virtual plane included the intraoperative surgical position of the robotic instruments, as surgical tools are placed at the labial commissures of the mouth. On this oblique view, point B was the same posterior palatine point, but the points C, E, and A changed into C′, E′, and A′, respectively, the parasagittal anterior palatine point, the parasagittal mandibular point, and the parasagittal lowest sella turcica point (see **Figure 8D**). The (BE′) line was projected on the sella turcica, and we determined whether it was presellar, postsellar, or on point A′ of the sella. Moreover, the α′ angle was the angle between the BE′ and BC′ lines. A comparison of α and α′ angle was performed. Thus, we were able to virtually compare if a lateral access changed the sella exposure.

Finally, pneumatization of the sphenoid sinus was defined according to the three physiological states that are concha, presellar, and sellar sphenoid sinus [17].

As a factor of surgical feasibility, we chose the projection of the dental palatine (BE) line on the sella. Thus, we separated the patients into two groups: the "straight approach" group with a presellar projection and the "no straight approach" group (with projection on point A of the sella and postsellar projection). Our statistical analysis included the following tests: the Kolmogorov-Smirnov normality test, the F-test for equality of variances, and the Student's t-test for patients' characteristics and comparison according to straight approach.

3.2. Results

A total of 38 cerebral CT scans were performed; out of those, 30 exams were assessed (mean patients' age = 57 years old); 8 patients were excluded because their mouth aperture was inferior to 30 mm. For all patients, the average mouth opening, aka [DE], was 39.4 mm IC 95% [36–42.8] and the length of the palate, aka [BC], was 47.4 mm IC 95% [45.2–49.5]. The distance between the inferior incisors and posterior edge of the hard palate, aka [BE], was measured at 69.5 mm IC 95% [67–72]. The average distance between the posterior edge of the palate

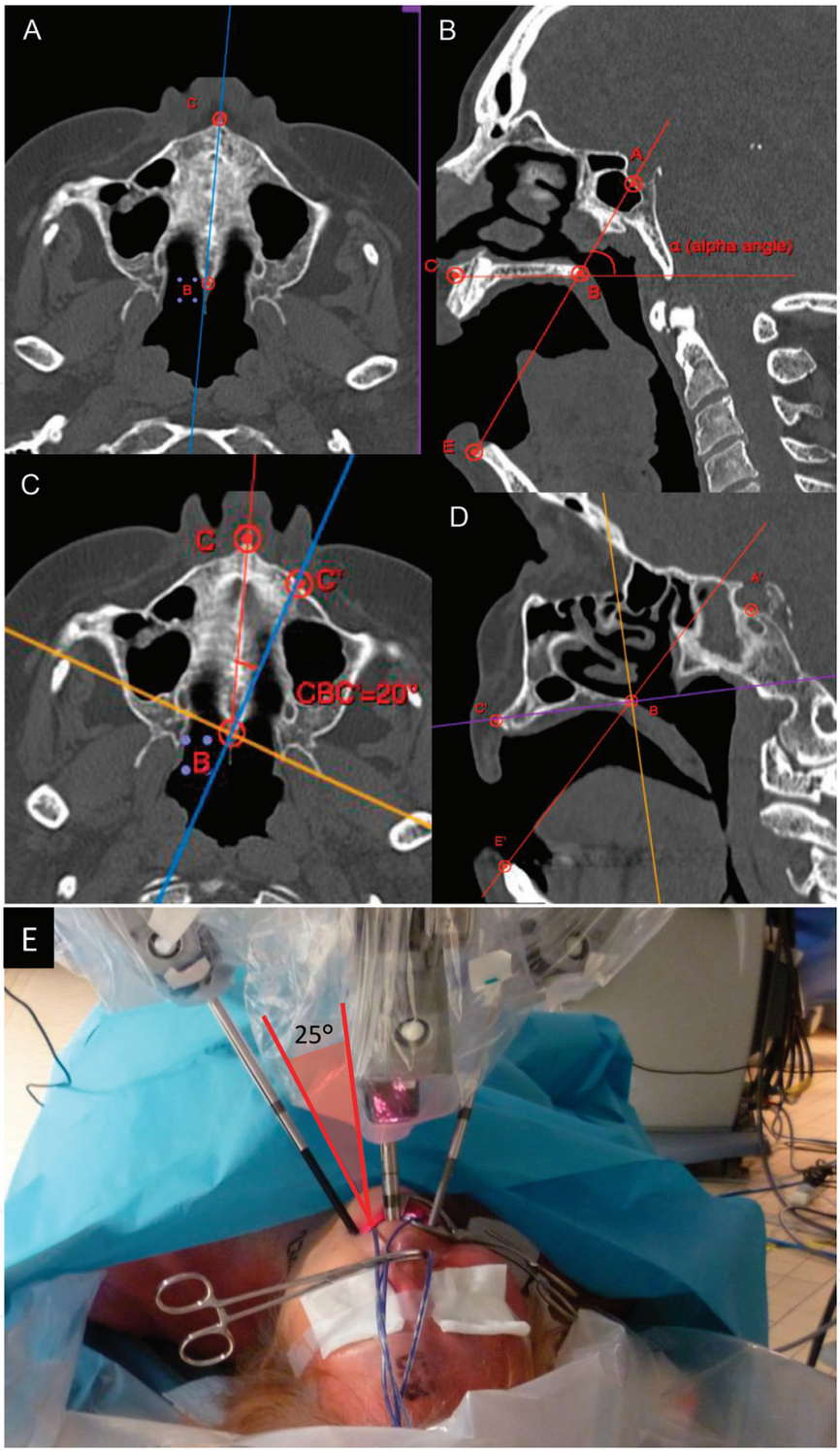

Figure 8. (A and B) Sagittal projections on midline: axial projection of the anterior maxillary point (point C) and the posterior palatine point (point B) and the midline sagittal view, the α (alpha angle) on the midline, determined as the angle between the BE line and the BC line. (C) and (D) Sagittal projections with lateral rotation of 25°. Axis rotation defined a parasagittal anterior maxillary point (point C′) and the parasagittal view with the parasagittal mandibular point (point E′) and the parasagittal sella turcica point (point A′). The posterior palatine point is fixed. (E) Photograph from cadaveric dissection of TORS at the bedside of the cadaver. The robotic instruments are placed into the oral cavity with a 25° angle (represented with a red triangle) between the endoscope at the midline and the dissector laterally [15].

[DE] mouth opening value (mm)	Sensitivity (%)	Specificity (%)
36.0	100.0	58.3
38.7	83.3	58.3
38.9	**83.3**	**70.8**
39.4	66.7	75.0
43.2	66.6	83.3
44.8	50.0	87.5
52.6	16.6	100.0

Table 1. Sensibility and specificity of mouth opening [DE] to predict the straight approach feasibility [15].

and the sella, aka [AB], was 43.1 mm IC 95% [41.5–44.7]. In our series, 2 patients (6%) had a presellar sinus and 28 patients (94%) had a sellar sphenoid sinus; we did not find any patient with concha sphenoid sinus.

Concerning our study of (BE) line projections on the sella, we described some dramatic changes between the midline plane and oblique plane. We found that 40% of patients (n = 12) had a (BE) line projection that moved forward when studied in the oblique plane, from the projection on A point to the presellar projection. Additionally, both angles, alpha α and α′, were significantly different ($p < 0.05$), respectively, 59.3° IC 95% [56.1–62.4] and 64.7° IC 95% [62.1–67.3]. It tends to show that the axis of the instruments at the labial commissure of the mouth opened the working angle to the skull base.

Regarding our straight approach feasibility hypothesis, the only significant predictive factor was the spontaneous mouth opening [DE] ($p < 0.05$). We also observed that a mouth opening of 38.9 mm is sufficient to obtain a sensitivity of 83% and a specificity of 70.8% to predict our straight approach hypothesis (see **Table 1**).

Consequently, these data emphasized that the physiological maximal mouth opening could be an excellent predictive factor for feasibility of TORS. However, it seemed obvious that patients suffering from trismus could not be included in the further clinical study.

4. Clinical study

4.1. Methods

This prospective clinical study confirms the accessibility of the sella with TORS. It was conducted after validation of the French ethic committee and registration in Clinical Trials NCT02743442. The patients were referred to our institution, Rothschild Foundation, Paris, after the discovery of the sellar tumor, mostly revealed by visual symptoms. Once prolactinoma was excluded, surgical removal was decided, and the patient was informed of dedicated

potential TORS risks (mastication difficulties, temporomandibular pain, hypernasal speech, and sore throat). A preoperative "open mouth" skull base CT scan was performed to envision the accessibility of the sella, as previously described [15]. The setup of the OR was the same than in our cadaveric study (see **Figure 1**). The only difference was that we used a da Vinci SI HD 4 arms system (Intuitive Surgical®, Sunnyvale, CA, USA). A general anesthesia was performed with the intubation placed on the left labial commissure.

The four surgical phases were the same as described above in the cadaveric work, except that a few modifications are described in the following lines.

4.1.1. Mucosal time

Mucosa of the posterior cavum was dissected into a "U-shaped" flap, instead of a caudal base flap (as in **Figure 3**), because we anticipated the possibility to raise the flap into the sella in case of CSF leak. During the next phases, this flap was positioned in the right choanae to facilitate sphenoidal approach.

4.1.2. Sphenoid time

The drilling of the key point was performed with a Midas Rex® Legend Stylus®, which offered an angled handpiece. Moreover, we used some diamond matchstick burs.

4.1.3. Sellar time and adenoma removal

For the dural opening, we prefer a CO_2 flexible Laser (Luminis®) guided by the robotic instruments rather than the monopolar cautery of the system. We must remind the reader that the da Vinci system has no dedicated instruments for pituitary surgery, so that the tumor removal was performed with curettes by the neurosurgeon at the patient's side (see **Figure 9**).

4.1.4. Closure

After removal, oxidized regenerated cellulose was placed against the sellar wall, and the mucosal flap was reapplied and sometimes glued. We did not try to suture the flap in the clinical trial, because preliminary works were mitigated.

Outcome measures included several criteria, such as preoperative data (i.e., visual function, radiological features of the tumor, open mouth CT scan data), intraoperative observations (i.e., exposure quality on the cavum and the sella, CSF leak occurrence, operative time for each phase, mucosal lesions in the oral cavity at the end of the procedure), and postoperative data. The latter were divided into two categories: TORS side effects (mastication dysfunction, temporomandibular pain, hypernasal speech, sore throat) and usual pituitary adenoma surgery outcomes/complications (vision status, CSF leak, meningitis, diabetes insipidus, hypopituitarism).

4.2. Results

Preoperative clinical data: a total of seven patients were included (five females, two males; mean age 46 years old). All presented with visual disturbance explained by bitemporal hemianopsia, except one patient who was operated on regarding the growth of his sellar tumor.

http://dx.doi.org/10.5772/intechopen.81048

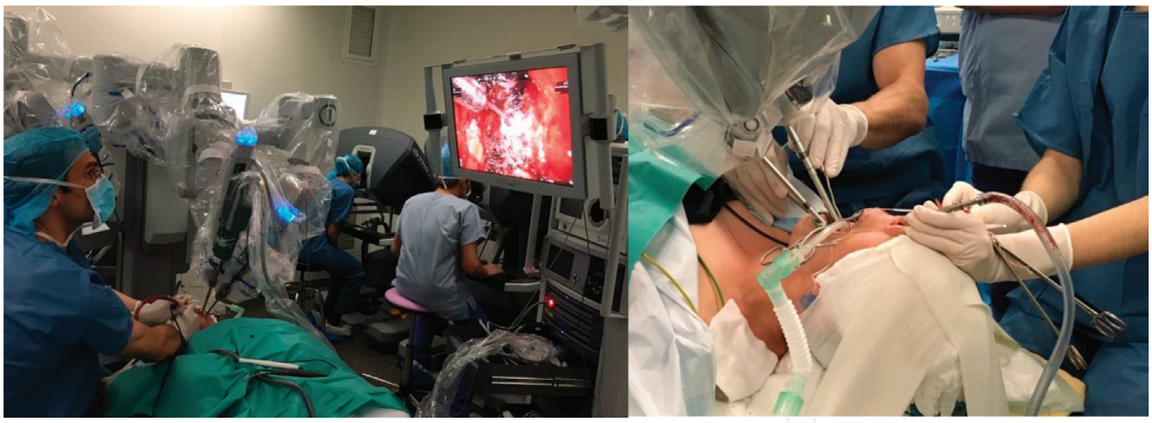

Figure 9. Operative views during the sphenoid and sellar times. The neurosurgeon (DC) performs the drilling at the bedside with his two hands placed at the labial commissure. An additional suction can be placed in the nasal cavity [16].

Preoperative radiological data: concerning radiological findings, five tumors were partially or totally cystic, and two were totally solid. All tumors but one had a suprasellar extension, which was responsible of the visual field defects. The mean size of the tumors' largest dimension was 29 mm (min 21, max 39). Preoperative open mouth CT scan revealed that all patients had a well-pneumatized sphenoid sinus (aka sellar type) and that the projection lines on the sella (see above) were divided into two presellar, three sellar, and two postsellar.

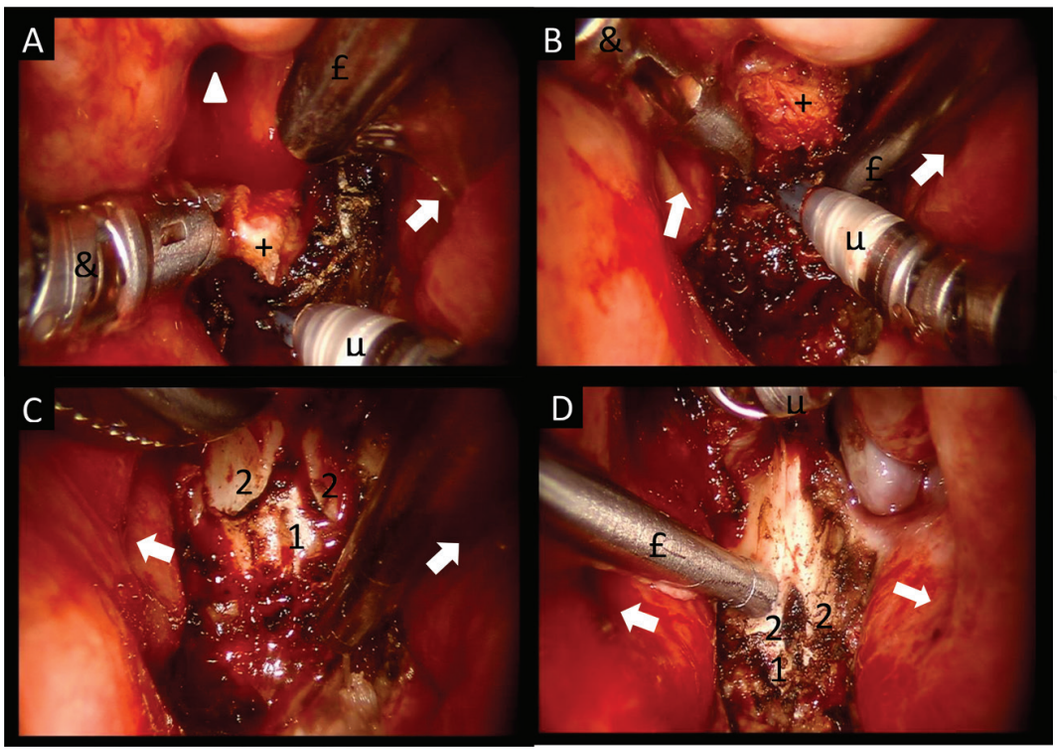

Figure 10. Intraoperative view at the console during mucosal time. (A and B) The mucosal flap (+) is progressively dissected and retracted upward using the Maryland dissector (&) and the monopolar cautery (μ) (patient n°1). (C) Visualization of the junction between the vomer, with its two alae (2), and the sphenoid bone (1) (patient n°1). (D) Suction (£) showing the key point to enter the sphenoid sinus (patient n°2). White triangle: right choanae; white arrows: Eustachian tubes [16].

Intraoperative data: the visualization of the cavum was good in all cases. However, we report one case in which the operative corridor was narrowed because of a thick mucosa. The mucosal flaps were dissected using the robot and reapplied at the end of surgery, except in one case as the flap was too retracted by the monopolar dissection. The key point at the junction between the vomer and the sphenoid was well identified in all cases (see **Figure 10**).

The sphenoid drilling allowed a penetration into the sphenoid sinus in all cases with a unique inferosuperior direction (see **Figure 11**).

The visualization of the sella was good, and the opening of the sella allowed reaching the tumor in all cases. Then, the removal quality depended on the tumor consistency. If the tumor was cystic (n = 5), the fluid drained off easily, and the curettage of solid component was quite easy. If the tumor was totally solid (n = 2), the removal was very hard because of two factors: (1) the surgery was very hemorrhagic, and we hypothesize that the position of the head was a possible reason; (2) the da Vinci system has no dedicated instruments such as curettes. This issue led to a partial removal, and patient n°5 had to be reoperated on via endonasal approach.

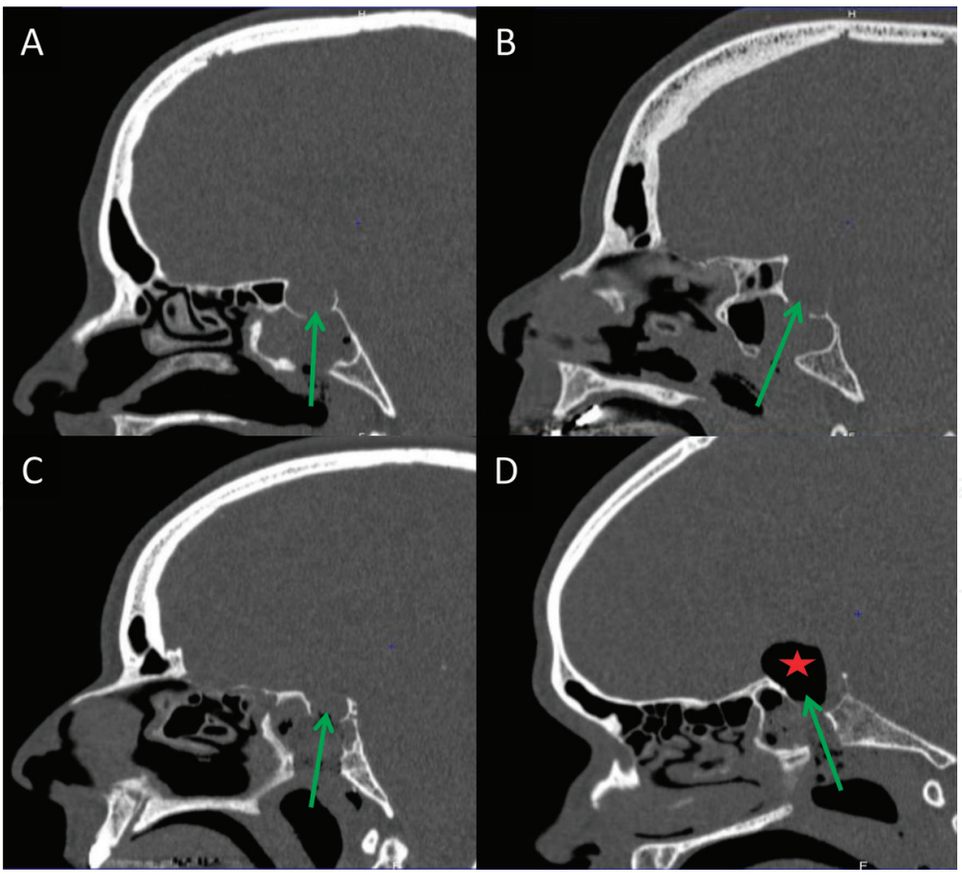

Figure 11. Postoperative brain CT scans at day 1 showing the inferosuperior approach of the sella with green arrows (A, B, C, and D for patients n°1, 2, 3, and 4, respectively). Red star indicates postoperative pneumocephalus in the pituitary fossa for patient n°4 [16].

http://dx.doi.org/10.5772/intechopen.81048

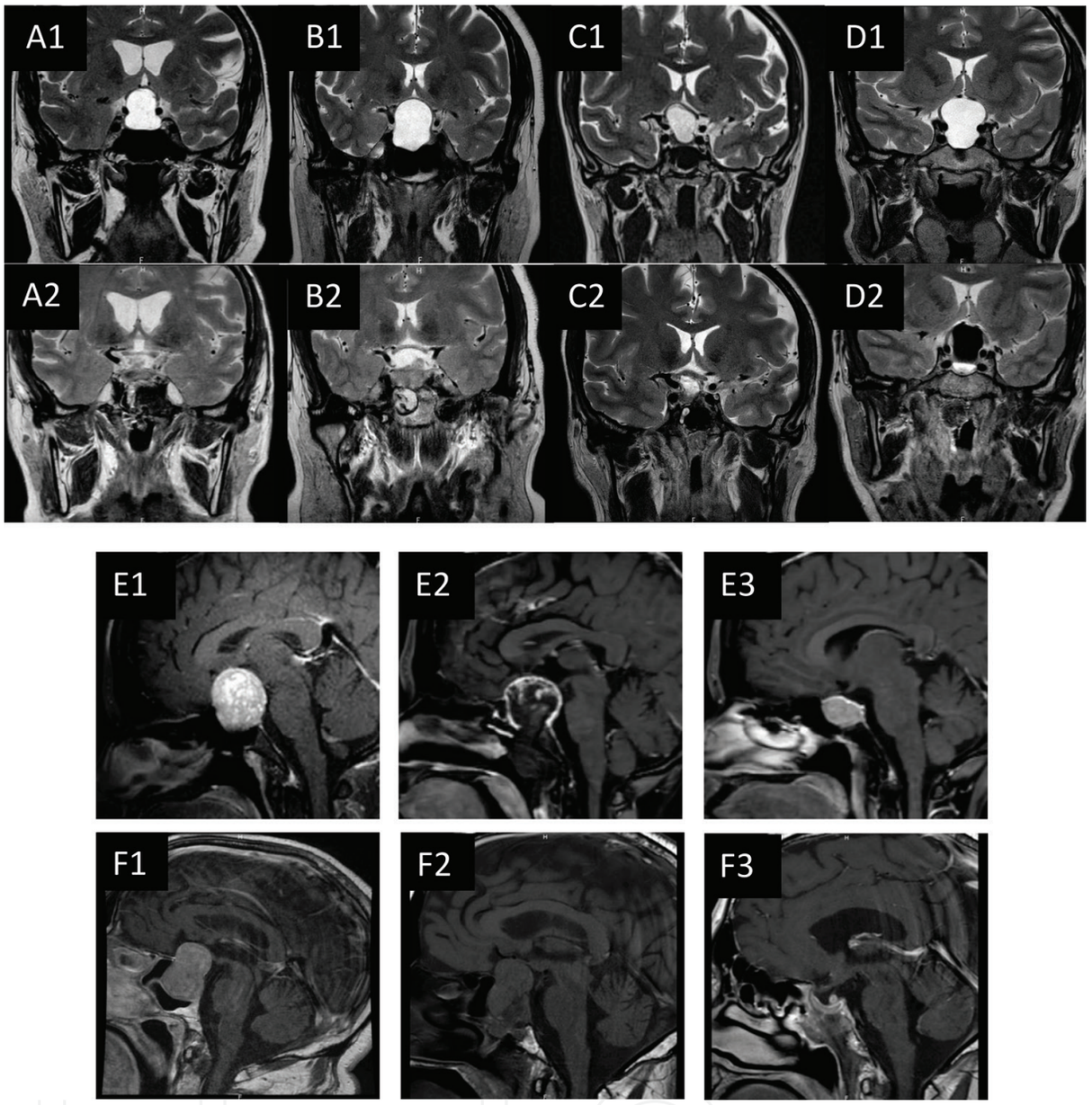

Figure 12. Upper figure shows coronal T2-weighted brain MR imagings, preoperatively (1) and postoperatively at day 1 (2). A, B, C, and D for patients n°1, 2, 3, and 4, respectively. For patient n°4, postoperative imaging (2D) shows intrasellar hyposignal corresponding to pneumocephalus [16]. Lower figure shows patient n°5 and 6, respectively, E and F. E1 preoperatively, E2 postoperatively at day 1 with hematoma within the sella, E3 postoperatively at 1 month with a resorption of the hematoma, and the chiasmatic decompression; F1 preoperatively, F2 postoperatively at day 1 with a partial reduction of the tumor, and F3 postoperatively after the second endonasal surgery.

At the end of the procedures, we observed three minor mucosal lip lesions (because of the drilling handpiece at the labial commissure) and two minor mucosal lesions next to the uvula (because of the loops to retract the soft palate).

Postoperative data: at 1 month after surgery, all patients have a better vision status. No rhinologic disturbance was noted. We reported the following TORS side effects: sore throat (n = 7) and hypernasal speech (n = 5). Fortunately, these symptoms were transient (approximately

3–5 days). One patient had an otitis media; we hypothesized that the reason could be a secondary constriction of the Eustachian tubes close to the dissected flap. We reported the following complications of sellar surgery: CSF leak (n = 1, resolved after lumbar puncture), diabetes insipidus (n = 2), and hypopituitarism (n = 1).

Regarding the postoperative MRI, we had good results about cystic lesions, but the removal quality was poor for the two solid tumors (see **Figure 12**).

Finally, we reported three pathological confirmations of gonadotroph adenomas. The other lesions were mainly cystic without diagnoses.

5. Conclusion

From this innovative TORS for sellar tumors, we can emphasize some promising results on cystic tumors, in a minimally invasive perspective because the side effects were minor and transient. The 3D visualization is very good, and the maneuverability of the robotic instruments is satisfying even in narrow spaces. Moreover, we think that this inferosuperior approach of the sella could bring interesting considerations for large suprasellar extension. However, we must comment on the lack of specific neurosurgical instruments in the da Vinci robot and the poor removal quality regarding solid pituitary adenomas, even if the tumors were reached in all cases.

Acknowledgements

We thank Prof. Lot for his general support regarding this project from the beginning to the last patients. We also thank Antoine Missistrano whose surgical assistance and general help were precious. We thank Wendy Gold for English corrections.

Conflict of interest

We declare no conflict.

Author details

Dorian Chauvet[1]* and Stephane Hans[2]

*Address all correspondence to: dchauvet@for.paris

1 Neurosurgery, Rothschild Foundation, Paris, France

2 Head and Neck Department, Hopital Européen George Pompidou, Paris, France

References

[1] Liu JK, Das K, Weiss MH, Laws ER Jr, Couldwell WT. The history and evolution of transsphenoidal surgery. Journal of Neurosurgery. 2001;**95**:1083-1096

[2] Yates DR, Vaessen C, Roupret M. From Leonardo to da Vinci: The history of robot-assisted surgery in urology. BJU International. 2011;**108**:1708-1713

[3] Advincula AP, Song A. The role of robotic surgery in gynecology. Current Opinion in Obstetrics & Gynecology. 2007;**19**:331-336

[4] Carrau RL, Prevedello DM, de Lara D, Durmus K, Ozer E. Combined transoral robotic surgery and endoscopic endonasal approach for the resection of extensive malignancies of the skull base. Head & Neck. 2013;**6**:351-358

[5] Hans S, Delas B, Gorphe P, Ménard M, Brasnu D. Transoral robotic surgery in head and neck cancer. European Annals of Otorhinolaryngology, Head and Neck Diseases. 2012;**129**(1):32-37

[6] Hans S, Hoffman C, Croidieu R, Vialatte de Pemille G, Crevier-Buchman L, Monfrais-Pfauwadel MC, et al. Evaluation of quality of life and swallowing in patients with cancer of the oropharynx treated with assisted transoral robotic surgery. Revue de Laryngologie Otologie Rhinologie. 2013;**134**:49-56

[7] Hans S, Jouffroy T, Veivers D, Hoffman C, Girod A, Badoual C, et al. Transoral robotic-assisted free flap reconstruction after radiation therapy in hypopharyngeal carcinoma: Report of two cases. European Archives of Oto-Rhino-Laryngology. 2013;**270**:2359-2364

[8] Lee JY, O'Malley BW, Newman JG, Weinstein GS, Lega B, Diaz J, et al. Transoral robotic surgery of craniocervical junction and atlantoaxial spine: A cadaveric study. Journal of Neurosurgery. Spine. 2010;**12**:13-18

[9] Lee JY, O'Malley BW Jr, Newman JG, Weinstein GS, Lega B, Diaz J, et al. Transoral robotic surgery of the skull base: A cadaver and feasibility study. ORL: Journal for Otorhinolaryngology and Its Related Specialties. 2010;**72**:181-187

[10] Yang MS, Yoon TH, Yoon DH, Kim KN, Pennant W, Ha Y. Robot-assisted transoral odontoidectomy: Experiment in new minimally invasive technology, a cadaveric study. Journal of Korean Neurosurgical Association. 2011;**49**:248-251

[11] Lee JY, Lega B, Bhowmick D, Newman JG, O'Malley BW Jr, Weinstein GS, et al. Da Vinci robot-assisted transoral odontoidectomy for basilar invagination. ORL: Journal for Otorhinolaryngology and Its Related Specialties. 2010;**72**:91-95

[12] Marcus HJ, Hughes-Hallett A, Cundy TP, Yang G-Z, Darzi A, Nandi D. Da Vinci robot-assisted keyhole neurosurgery: A cadaver study on feasibility and safety. Neurosurgical Review. 2015;**38**:367-371

[13] Crockard HA. The transoral approach to the base of the brain and upper cervical cord. Annals of the Royal College of Surgeons of England. 1985;**67**:321-325

[14] Chauvet D, Missistrano A, Hivelin M, Carpentier A, Cornu P, Hans S. Transoral robotic-assisted skull base surgery to approach the sella turcica: Cadaveric study. Neurosurgical Review. 2014;**37**:609-617

[15] Amelot A, Trunet S, Degos V, André O, Dionnet A, Cornu P, et al. Anatomical features of skull base and oral cavity: A pilot study to determine the accessibility of the sella by transoral robotic-assisted surgery. Neurosurgical Review. 2015;**38**:723-730

[16] Chauvet D, Hans S, Missistrano A, Rebours C, Bakourri WE, Lot G. Transoral robotic surgery for sellar tumors: First clinical study. Journal of Neurosurgery. 2017;**127**:941-948

[17] Hamberger CA, Hammer G, Marcusson G. Experiences in transantrosphenoidal hypophysectomy. Transactions of the Pacific Coast Oto-Ophthalmological Society Annual Meeting. 1961;**42**:273-286